Journal of Environmental Management 95 (2012) S175–S181

Contents lists available at ScienceDirect

Journal of Environmental Management

journal homepage: www.elsevier.com/locate/jenvman

The performance of natural clay as a barrier to the diffusion of municipal solid waste landfill leachates

Jaime Cuevas [a,*], Ana I. Ruiz [a], Isabel S. de Soto [a], Teresa Sevilla [b], Jesús R. Procopio [b], Pilar Da Silva [b], Mª Jesús Gismera [b], Mercedes Regadío [a], Nicanor Sánchez Jiménez [b], Manuel Rodríguez Rastrero [a], Santiago Leguey [a]

[a] Departamento de Geología y Geoquímica, Universidad Autónoma de Madrid, Facultad de Ciencias, Campus de Cantoblanco, 28049 Madrid, Spain
[b] Departamento de Química Analítica y Análisis Instrumental, Universidad Autónoma de Madrid, Facultad de Ciencias, Campus de Cantoblanco, 28049 Madrid, Spain

ARTICLE INFO

Article history:
Received 30 September 2009
Received in revised form
7 January 2011
Accepted 23 February 2011
Available online 21 March 2011

Keywords:
Clay barriers
Landfill
Contaminant transport
Anion diffusion

ABSTRACT

In this paper, the diffusion of solutes in natural clay from a concentrated solution consisting primarily of ammonium, sodium and chloride ions at a pH level of 8 was studied and was based on an existing 20-year-old landfill. Contaminant transport through clay liners was predicted using transport and reaction geochemical codes to help explain the experimental data. The model predicted the chloride anion diffusion and cation exchange processes for three different experiments: (1) small-scale interactions in compacted clay, (2) 1:1 European Union (EU) Directive demonstration experiments (0.5-m-thick clay barrier), and (3) analysis of a bore hole with core recovery drilled in an old landfill located above a similar type of clay as that studied in (1) and (2). Orders of magnitude between 10^{-10} and 10^{-9} m^2 s^{-1} were used for the apparent diffusion coefficient to fit the chloride profiles at the different scales; however, at larger space and time scales, diffusion was retarded due to the presence of more consolidated, non-mechanically disturbed clay materials at large depths in a natural clay-rock emplacement.

1. Introduction

The technical requirements for municipal waste landfills in the European Union (EU) are given in the Council Directive 1999/31/EC and decision (2003/33/CE), which established the requirement of a geological barrier thickness of at least 1 m, with a hydraulic conductivity of $1 \cdot 10^{-9}$ m s^{-1}. If a geological barrier does not naturally meet the conditions, a geo-synthetic barrier thickness of at least 0.5 m must be artificially created. Geological barriers are important because they confine waste and buffer the hazardous leachates; thus, they are a key factor for upholding the protection and safety objectives of waste disposal (Bilitewski et al., 1997; Savage, 1995; Astudillo, 2001).

Natural clay materials have a very low permeability because of their small pore sizes and complex porous structures. Their high specific surface areas allow for strong physical and chemical interactions to occur between fluids and dissolved species that are subjected to electrostatic repulsion, sorption and specific cation exchange reactions, and these interactions are responsible for retaining leachate components in landfills (Davis and Kent, 1990; Sposito, 1990; Stumm, 1992; Rowe et al., 1995; Sawney, 1996; Michael et al., 2002). Furthermore, clays impede fluid transport and retard the migration of solutes, which can be confirmed by correlating the predominance of clay under a landfill vessel with a natural pollution attenuation; for example, ammonium attenuation as a function of depth illustrates the role of clays in retardation of cations (National Groundwater and Contaminated Land Center, 2003).

The objective of our work was to perform a preliminary study of the transport of contaminants through natural clay material in municipal solid waste (MSW) landfills. A multi-scale experimental program was designed to help create the models and to compare the relevant parameters from the models, such as the diffusion coefficients, with the field data taken from a 20-year-old municipal landfill. In this study, the behavior of chloride, ammonium and sodium ions is discussed.

2. Materials and methods

2.1. Materials

Plastic clay from El Papiol (Barcelona, Spain) was selected because it has previously been used as a landfill liner in this region (Rogel et al., 2008). El Papiol clay has a heterogeneous mineralogy that is composed primarily of the main sheet silicates in the clay

* Corresponding author. Tel.: +34 91 497 30 47; fax: +34 91 497 49 00.
E-mail address: jaime.cuevas@uam.es (J. Cuevas).

0301-4797/$ – see front matter © 2011 Elsevier Ltd. All rights reserved.
doi:10.1016/j.jenvman.2011.02.014

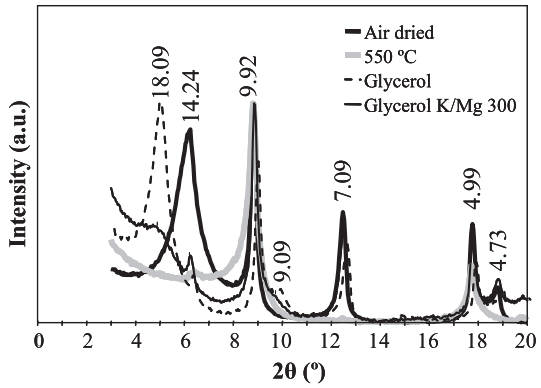

Fig. 1. XRD patterns (λ = Cu Kα) of <2 μm size fraction (clay size) of El Papiol clay. Several characterization treatments were performed (Moore and Reynolds, 1989; Malla and Douglas, 1987). Numbers are XRD reflection positions in Å (transformed from the reflection angle (θ) by the Bragg law (λ = 2d(Å)Sinθ). d: structural distance between parallel layers in the sheet-silicate structure; Glycerol: Glycerol solvated; Glycerol K/Mg 300: homoionized in K^+, heated to 300 °C and re-hydrated in Mg^{2+}-homoionized form; 550 °C and Air dried: heated or dried in the Mg^{2+} form.

mineral family (Brindley and Brown, 1984): illite (primarily), chlorite, kaolinite and smectite. The mineralogy was studied by X-ray diffraction (XRD) and was analyzed by random powder and oriented clay fraction (<2 μm) methods. Illite exhibited a 001 reflection at 10 Å and remained unchanged by glycerol solvation. However, the long d-spacing (14 Å) of the expandable clay (smectite) was modified upon solvation with glycerol (18 Å). The sharpness of the reflection and the collapse of the 14–18 Å structure under K^+ homoionization at 300 °C indicate that smectite is a highly charged, large-sized beidellite crystal, as shown in Fig. 1 (Malla and Douglas, 1987). The relatively low specific surface area determined for this clay (19 $m^2\ g^{-1}$) is in agreement with the sharpness of the clay mineral reflections (large-sized crystals imply a small surface area). Furthermore, the destruction of the 7-Å structure at 550 °C indicates the existence of kaolinite or iron-rich chlorite (Moore and Reynolds, 1989). Non-clay minerals, such as quartz, calcite, feldspars and iron oxide (hematite), represent approximately 40% of the bulk material (Table 1). The clay, which had a hydraulic conductivity of $5.2 \cdot 10^{-10}$ m s^{-1} for the optimum water content at the maximum density (10% H_2O; 2.0 g cm^{-3} dry density), was tested to satisfy the technical EU Directive requirements. Also, the total organic carbon content (TOC) was less than 0.01%.

Table 1 shows the mineralogical composition, the distribution of the exchangeable cations and the major ions extracted in a 1:5 solid/water ratio. The geochemical code PHREEQC 2.14 was used to fit the initial pore water of the clay and the initial distribution of the exchangeable cations. The code was run at fixed pH/Eh conditions, 8.5/pe = −4, in the clay. This pH level was measured at the clay-leachate interface in both the small- and EU demonstration-scale experiments. Also, the redox potential remained constant to prevent the bicarbonate reduction to methane, which occurs at pe < −5 at a pH level of 8.5.

The initial pore water composition was measured in a 1:5 aqueous extract with El Papiol Clay. A factor of 20 to concentrate the main ions (Cl^-, K^+ and Na^+) was calculated by accounting for the naturally compacted water in saturated clay (0.25 l H_2O/kg, saturation at 2.0 g/cm^3 dry density), and the aqueous extraction was obtained in a 1:5 solid to liquid ratio. The alkalinity was related to the calcite solubility, and the Mg^{2+} concentration was related to dolomite solubility. The cation Ca^{2+} was used to satisfy the charge balance. Then Na^+ was varied to approach the initial cation exchange equilibrium, and the model also included the main minerals present in the clay: montmorillonite, illite, quartz, calcite, dolomite and hematite.

A portion of the calcium and magnesium content was dissolved from carbonates when the aqueous extraction was performed. These cations, with a higher electric charge, displace Na^+ from the exchange complex. Thus, the Na^+ concentration in the pore water should be lower than the measured concentration.

2.2. Experiments

2.2.1. Small-scale diffusion experiments

The clay was compacted at its optimum water-saturated maximum density in a Teflon cylinder cell that had a height of 2.1 cm and a diameter of 7 cm. The cell was confined in a stainless steel mold, where fluid was forced to flow at either side of the disc through the Teflon porous membranes (<1 mm thickness under compaction, one filter at the top of the mold and the other filter at the bottom). The small thickness and large-sized pores of this membrane minimized the artifacts introduced in the diffusion experiments through the use of porous plates in the compacted clays (González et al., 2009). The fluid at each side was recycled to configure the pure diffusion experiment. Distilled water (2 L) flowed through the bottom filter for 2 months in one side. After 2 months, a synthetic leachate was recirculated through the top porous membrane for another 2 months. Electrical conductivity was measured on-line in the distilled water deposit. After 2 months of leachate diffusion, the clay sample was divided into 4-mm sections to determine the mineralogy and physical-chemical

Table 1
Mineralogical composition (weight %) and physical–chemical properties of El Papiol clay.

Mineralogical composition									
Clay minerals				Q	Fn	Fk	Cal	Dol	Other
T	K	I	S						
58	9	33	16	30	1	1	6	2	H, C
Physical–chemical properties									
	SUP	ΣEC	Exchangeable cations				CEC		
			Na^+	K^+	Mg^{2+}	Ca^{2+}			
Exp.	19 ± 1	20 ± 2	0.25 ± 0.05	0.3 ± 0.1	3.4 ± 0.3	14 ± 1	16 ± 1		
Model	–	–	2.0	0.1	2.5	11.0	15.6		
	Soluble ions							pH	
	Na^+	K^+	Mg^{2+}	Ca^{2+}	Cl^-	SO_4^{2-}	HCO_3^-		
Exp.	1.56 ± 0.44	0.11 ± 0.01	–	0.69 ± 0.11	0.56 ± 0.29	0.19 ± 0.08	–	8.5	
Model	20.00	2.43	1.00	0.5	12.39	–	0.5	8.5	

T: Total clay; K: kaolinite; I: Illite; S: Smectite; Q: quartz; Fn, Fk: sodium, potassium feldspar; Cal: calcite; Dol. Dolomite; H: Hematite; C: Chlorite. SUP: Specific surface measured by the BET N_2 adsorption method ($m^2\ g^{-1}$). Σ EC: sum of exchangeable cations. Na^+, K^+, Mg^{2+} and Ca^{2+}: exchangeable cations (cmol(+)/Kg). CEC: Cation exchange capacity (cmol(+)/Kg). Na^+, K^+, Mg^{2+}, Ca^{2+}, Cl^-, SO_4^{2-} and HCO^{3-} : soluble cations (mmol/l) in a 1:5 solid/water aqueous extract. Model: initial conditions fitted with PHREEQC (Pakhurst and Appello, 1999) modeling.

properties of the samples, as was reported for the natural clay in Table 1. The synthetic leachate (L1 in Table 2, Cuevas et al., 2009) was a simplified formulation of the landfill leachate obtained from the El Garráf (Barcelona) Landfill (L2 in Table 2, Cuevas et al., 2009). The synthetic leachate had a composition of an aged landfill leachate reacting at the methanogenic stage (Williams, 1998; Pivato and Raga, 2006).

2.2.2. EU Directive (0.5-m-) scaled diffusion experiments

Compacted clay columns with lengths of 0.5 m were packed in 0.25-m diameter, 1-m length methacrylate cells, which resulted in a dry density of 2.0 g/cm^3. Two cells were prepared: (1) one with distilled water and (2) one with the addition of a landfill leachate obtained from a collector pipe in the El Garráf (Barcelona) Landfill (L2 in Table 2). The clay was held in contact with the solutions for six months. The contact between the clay and the liquid displayed an altered zone of 2–5 cm that had expanded in relation to the bulk column. Samples were taken at 2-(M01), 4-(M02) and 6-(M03) cm depths, measured from the point of liquid contact (Fig. 2). Another sample was taken from a section at 40–45 cm, measured from the cell bottom with an average depth of 10 (M09) cm from the point of liquid contact. These samples were analyzed to determine their mineralogy, physical–chemical properties and heavy metal ions. In addition, the entire column was tested every 5 cm for chlorides and sulfates to study the ionic transport through the clay.

2.2.3. Sampling of a clay bed under an old landfill

A 20-year-old landfill, which lay on El Papiol geological formation, was drilled up to a 3-m depth from the clay-waste contact. The clay was located below 16 m of waste. The leachate in the waste-clay contact was primarily inorganic, with a sodium chloride composition in the range of 0.4 mol l^{-1} (L3 in Table 2) and a lower organic content and a lower pH level (7.2) than the El Garráf Landfill.

2.3. Analytical methods

The mineralogy was studied by XRD after dismantling the experiments or from the samples from the drilled cores. To semi-quantify the minerals from the bulk sample, the procedure proposed in the UNE 22-161-92 was used. The specific surface area was determined by the Brunauer, Emmett and Teller method (BET) by multipoint N_2 adsorption using a Micromeritics® GEMINI V, after degassing under a N_2 flow for 18 h at 90 °C (UNE 22-164/94). For the surface chemistry analysis, the exchangeable cations were extracted from the clay at room temperature as described by Thomas (1982). The cations were analyzed with the following tools: Na^+ and K^+ using a Buck Scientific™ PFP-7 flame photometer; Ca^{2+} and Mg^{2+} by an ICP-MS (ELAN 6000, PERKIN ELMER™); and NH_4^+ by ion selective potentiometry (ORION™ 9512 Ammonia Gas Sensing Electrode). The cation exchange capacities (CEC) of the original clays were determined at room temperature by Na^+ homoionization ($Na-COO-CH_3$ 1 M, pH = 8) and Mg^{2+} displacement ($MgNO_3 \cdot 5H_2O$ 0.5 M, pH = 5), which was used by Rhoades (1982).

Chloride and sulfate anions were measured by ion chromatography (Metrohm™ 761 Compact IC) in aqueous extracts (1:10 solid:liquid ratio). The suspension was soaked for 2 h and was then left to settle for 24 h. The supernatant was extracted and filtered. To determine the heavy-metal ion content in the uppermost zone of the clay column (EU Directive experiments), the dried clays were digested in aqua regia (6 ml of HCl and 2 ml of HNO_3) inside a microwave oven (12 min at 1000 W in PFA vials). The drill cores were treated in the same way. The suspensions were filtered and analyzed by atomic absorption spectrometry (AAS) (Unicam™ Solaar M). The same analysis was also performed in the leachate collected before the clay columns were sampled.

Table 2
Characteristics of the different leachates used as reference for modelling calculations.

	Synthetic Leachate (L1)	El Garraf Leachate (L2)	Old Landfill Leachate (L3)
pH	7.78	8.60	7.20
CH_3COO^-	0.10	0.039	0.025
HCO_3^-	0.15	n.d.	n.d.
Cl^-	0.25	0.253	0.400
NH_4^+	0.25	0.254	0.025
Na^+	0.25	0.196	0.450
K^+	–	0.059	0.012
Ca^{2+}	–	1.25×10^{-4}	–
Mg^{2+}	–	0.005	0.012
Cu	–	9.45×10^{-7}	2.36×10^{-6}
Zn	–	4.89×10^{-6}	4.89×10^{-6}
Pb	–	1.01×10^{-6}	2.08×10^{-6}
Cd	–	$< 1.78 \times 10^{-7}$	1.78×10^{-7}
Fe	–	4.83×10^{-4}	–

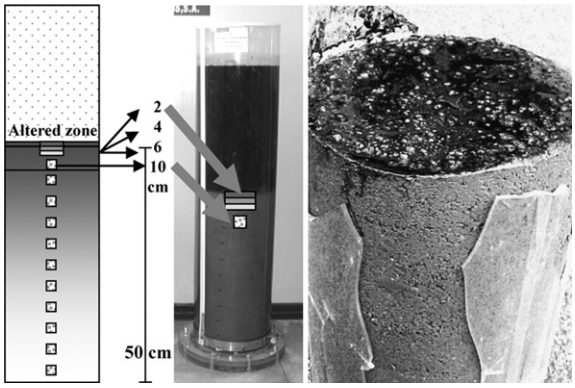

Fig. 2. Detail of "Biofilm" formation and sampling of the column experiments, with "El Garráf" leachate.

3. Results and discussion

3.1. Small-scale diffusion experiments

A significant diffusion of soluble salts was detected after the beginning of the synthetic leachate circulation (Fig. 3). A diffusion reaction model was used to simulate the diffusion of chloride and the cation exchange processes. The initial conditions for the model were described for the pore-water calculation in the natural clay (Table 1). The code PHREEQC (Parkhurst and Appelo, 1999) was used in the simulation. The simulation was carried out in two steps during a 2 month duration; first, distilled water was forced to circulate at the bottom of the cell, and second, the synthetic leachate circulated at the top. The fluid volumes in the simulation were 0.125 L for the leachate container, 0.01 L for the pore water (25% porosity in the clay) and 1 L for the water deposit. A trend line was obtained to explain the increase of the electrical conductivity in the water deposit with an apparent diffusion coefficient of $2 \cdot 10^{-9}$ m^2 s^{-1}, which is within the order of magnitude of the values obtained by Barone et al. (1989) (7.5 10^{-10} m^2 s^{-1}) in similar experiments performed with a compacted, carbonate-rich, clay-like soil (51% clay minerals).

In addition to the diffusion of the soluble components in the solution, other changes were determined for the solutions and the clay material. The pH level increased from 7.8 to 9.2 in the leachate deposit, and subtle mineralogical changes were observed in the clay slice in contact with the leachate port. When upon contact with the leachate, the amounts of calcite ($CaCO_3$) and dolomite

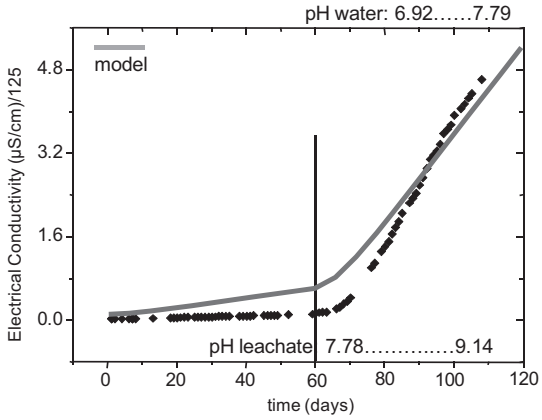

Fig. 3. Electrical conductivity (EC) profile in the small cells diffusion experiment (dots) transformed to chloride concentration (NaCl equivalence using molar electrical conductance = 125 Ω^{-1} cm^2 mol^{-1}). Modeling of chloride concentration with an apparent diffusion coefficient: $2\cdot10^{-9}$ m^2 s^{-1} pHs correspond to the initial and final pHs front stage 1 to stage 2 of the diffusion experiment.

($CaMgCO_3$) increased and decreased around 1%, respectively. This result can be explained by the formation of acetate complexes with calcium (Hatch, 2008) that would maintain the calcium in the solution which favors the precipitation of calcite. Alternatively, the precipitation of carbonates can be caused by the fermentation of acetate, which adds carbonate and increases the pH level (VanGulck et al., 2003), but the concentration of acetate was not measured. The physical–chemical properties, namely the CEC and specific surface area (SUP), did not change, which made ammonium the major exchangeable cation with a mole fraction greater than 0.8 of the CEC throughout the entire clay disc. In fact, chemical gradients were not observed inside the clay disc due to the long diffusion time of the experiment, which allowed the leachate fluid to equilibrate within the clay.

Fig. 4a shows the constant chloride profile across the thickness of the clay. The concentration in the clay was lower than predicted by the diffusion model, which predicted a sharp decrease of chloride in the leachate. The exclusion of chloride from this smectitic-rich clay can explain this result (Derrington et al., 2006). However, the diffusion of chloride into water was properly modeled.

The resulting ammonium concentration in the exchange complex was set to 2 cmol(+)/kg by the model (Fig. 4b). This low value, compared with the experimental value (10 cmol(+)/kg), was a result of the significant amount of Ca-montmorillonite (7%) or dolomite (1%) dissolution needed for the equilibrium calculations between the clay and the pore water. This calculation cannot be avoided in an equilibrium reaction model when the actual mineralogy must be considered. Calcium was incorporated into the exchangeable positions rather than ammonium. To overcome this problem, kinetic constraints must be used to control the mineral dissolution. The concentration of sodium was maintained near the initial values in the clay.

Table 3
Values of depth (*D*, m), pH, chloride concentration in fluid and fluid pores (Cl^-), exchangeable cations cmol(+)·Kg^{-1}): Na^+, K^+, Mg^{2+} and Ca^{2+}, specific surface (SUP, m^2 g^{-1}) and total organic carbon (TOC, C %) in the 0.5 m UE directive experiments with El Papiol clay. L1: distilled water; L2: landfill leachate.

	D	pH	Cl^-	Σ EC	Na^+	K^+	Mg^{+2}	Ca^{+2}	NH_4^+	SUP	TOC
L1											
Fluid		7.8	0.3								
M01	0.01	8.7	2.7	28	0.3	0.6	5.2	22	0.1	21	0.2
M02	0.03	8.7	3.2	31	0.9	1.4	6.7	22	–	19	0.2
M03	0.05	8.7	3.7	33	0.7	1.2	6.5	25	0.1	19	0.2
M09	0.1	8.7	3.5	19	0.5	0.4	4.5	13	–	20	0.2
L2											
Fluid		8.2	253.0								
M01	0.01	8.8	260.0	31	6.0	5.1	1.7	17	0.8	9	1.5
M02	0.03	9.0	216.0	34	6.1	6.1	4.4	13	4.7	12	1.0
M03	0.05	8.8	19.24	33	3.6	5.2	3.7	12	8.6	15	0.4
M09	0.1	8.7	14.67	40	1.8	2.1	2.9	28	6	16	0.4

Note: Additional information and data can be obtained from the reports summarized in Rogel et al. (2008).

3.2. EU Directive diffusion experiment

After six months, the physical–chemical parameters measured in the clay-leachate contact region from the experiments displayed strong similarities with those observed in the previous small cells. The pH value was above 8 in the leachate contact, and calcite also precipitated in small amounts at depths of 2–4 cm. Despite a high concentration of ammonium in the El Garráf leachate, this cation was not significant in the exchange complex of the M01 sample. This result was detected to a small extent in the small diffusion experiments and can be related to the formation of the clay-organic complexes at this contact region. In this region, a critical effect was observed where the specific surface decreased in the first 4 cm, which is related to the presence of organic cements (see TOC in Table 3). This result produces organic and inorganic clog particles and decreases the available surface area (Cuevas et al., 2009; Islam and Singhal, 2004; VanGulck and Rowe, 2004).

A diffusive chloride (major anion) front was produced, but its shape could not be modeled exactly; however, an apparent diffusion coefficient of $5\cdot10^{-9}$ m^2 s^{-1} (Fig. 5a) resulted in the best profile.

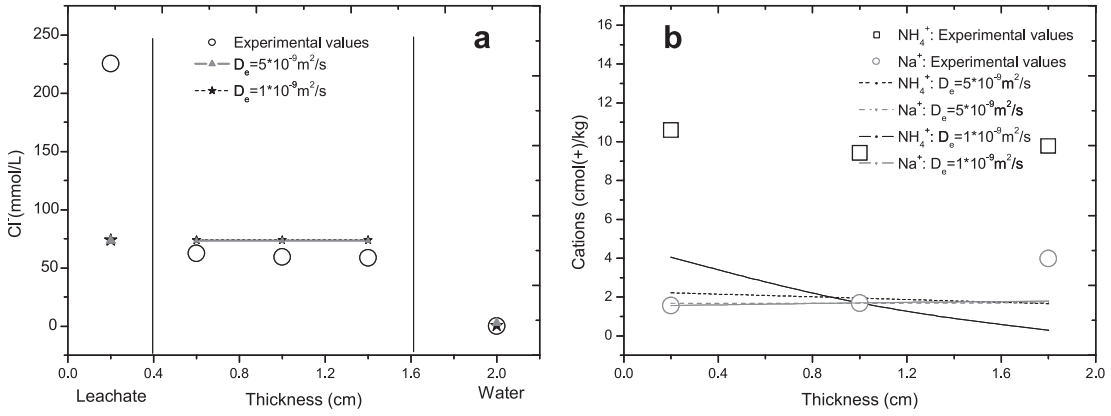

Fig. 4. Ions profiles *vs.* thickness of clay: a) chloride, b) ammonium and sodium.

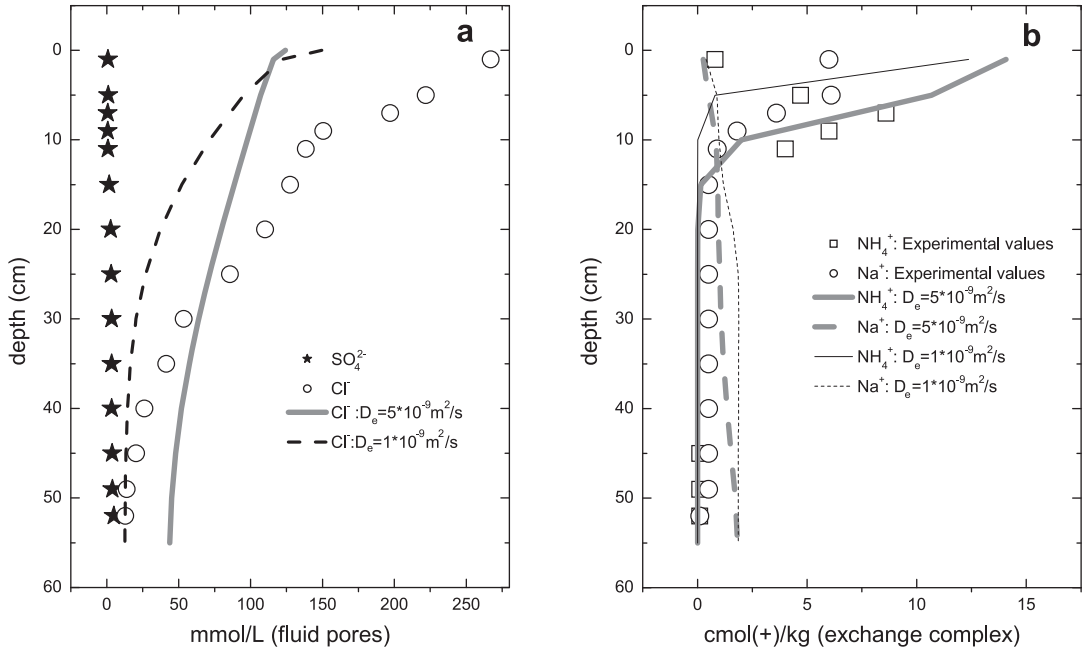

Fig. 5. Ions profiles *vs.* depth of UE directive column experiments: a) chloride and sulfate (concentration in pore water, mmol/L), b) ammonium and sodium (concentration in the exchange complex on a dry solid mass basis, cmol(+)/kg).

This diffusion coefficient was similar to the value from the small-scale experiments. However, the high content of chloride in the first 10–15 cm should be related to the density change produced by the overall 5- or 6-cm expansion of the 50-cm column, which affects the upper part of the column because higher quantities of the chloride solution are absorbed. The hydraulic conductivities of $1–10\cdot10^{-10}$ m s^{-1} at the hydraulic gradient equal to 1 should produce a solute front penetration of less than 3 cm in 10 months, which means that contaminant penetration in landfills should be studied where all the transport mechanisms are considered, not just the permeability.

An important detail in the column, although not modeled, is the sulfate reduction effect in the first 15 cm of depth (Fig. 5a). This effect is normally a reaction mediated by bacteria and precedes the methanogenic stage of the landfill organic matter degradation (Williams, 1998; Brun and Engesgaard, 2002), which establishes the basic pH level and the predominance of the inorganic ammonium-sodium chloride leachates. The basic pH levels and the precipitation of minerals can explain the low mobility of the heavy metal ions analyzed (Table 4). Heavy metals, such as Cu, Zn and Pb, migrate less than the soluble species due to the precipitation of carbonates (Yanful et al., 1988a,b). For example, in the Sarnia Landfill site, metals have diffused only 20 cm into the clay compared with 130 cm for chloride and sodium (Yanful et al., 1988b).

The modeling of exchangeable ammonium (Fig. 5b) predicted the increase of ammonium to a depth of 4–10 cm, but a strong buffering of the carbonate equilibrium produced a predominance of calcium and magnesium at greater depths. This buffering affected the sodium content in the exchange positions in the entire column because sodium has less selectivity than both ammonium and divalent cations. This case should also be studied in future works with the aid of a kinetics-based code that controls the mineral dissolution.

Table 4
Heavy metal ions (μg g^{-1}) in the clay-liquid contact (M01 samples).

Sample	[Zn]	[Cd]	[Pb]	[Cr]
Clay untreated	101.8	1.67	36.2	38.5
L1M01	107.8	1.35	38.6	38.5
L2M01	105.3	0.72	48.9	32.2

3.3. Clay bed under an old landfill

Regarding the pH level, the ammonium depletion at both the waste contact, the salt gradient and the observed physical–chemical parameters in the landfill clay (Table 5) displayed obvious similarities with the observed values of these parameters in the EU Directive 0.5-m experiments and even in the small-scale cells. However, different values of several parameters, such as the mineralogy and the specific surface, were observed. This difference is linked to the existence of an unconsolidated, less clay-rich material in the upper part of the base landfill clay. In this case, the upper clay-organic layer was not significant, as all the clays were less than 0.1% in the TOC.

The migration of sodium and ammonium up to 1.5 m below the waste occurred in the landfill after 20 years (Table 5). Similar data were found for Na and K migration in the Sarnia Landfill site after 16 years (Rowe, 1989).

Table 5
Selection of parameters tested in the drill cores form the old landfill with a base clay similar to El Papiol.

D	pH	EC	Cl^-	NH_4^+	Na^+	CEC	F	Cal	Do	SUP
1.25	8.6	11.30	201.8	0.38	6.88	18.65	46.7	28.1	0.3	16
3.75	8.7	11.22	150.4	0.36	7.52	14.91	50.4	27.2	0.4	20
6.25	8.6	11.22	158.0	0.58	7.20	13.80	55.1	24.6	0.6	17
8.75	8.6	10.70	116.1	0.57	6.99	20.34	53.4	26.6	0.8	20
17.5	8.7	10.47	126.2	0.66	5.82	18.30	41.9	30.5	1.2	18
65.0	8.9	10.00	124.6	0.41	8.13	21.77	62.2	12.8	3.6	28
115.0	8.7	6.10	50.4	0.24	3.91	25.39	75.5	7.9	3.0	31
155.0	9.2	0.807	6.0	0.10	1.46	22.83	59.9	14.1	5.0	31
225.0	9.2	0.815	2.8	0.13	2.03	24.45	74.3	9.7	3.5	39

D: Depth (cm). EC: electrical conductivity (mS cm^{-1}). NH_4^+ and Ca^{2+}: exchangeable cations (cmol(+)·Kg^{-1}). CEC: Cation exchange capacity (cmol(+)·Kg^{-1}). F: Total clay minerals; Cal: Calcite; Dol: Dolomite (%). SUP: Specific surface (m^2 g^{-1}). The complete data set obtained in the drilled cores is reported in the final report of the project: MMA: I+D+i A113/2007/3_02.6. La difusión de contaminantes en las barreras de vertederos urbanos y su evolución en el tiempo. Junio 2010.

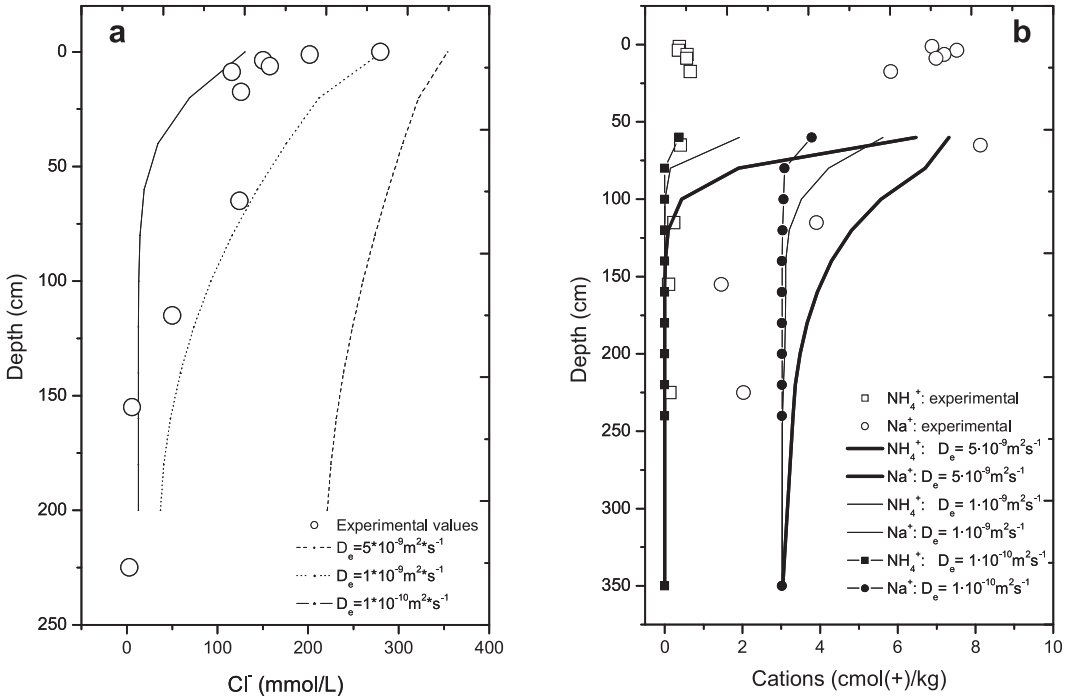

Fig. 6. Ions profiles *vs.* depth of landfill clay: a) chloride (concentration in pore water, mmol/L), b) ammonium and sodium (concentration in the exchange complex on a dry solid mass basis, cmol(+)/kg).

The modeled chloride diffusion at 20 years introduced a reduction of one order of magnitude for the apparent diffusion coefficient (10^{-10} m^2 s^{-1}, Fig. 6a). For the modeled cations (Fig. 6b), the diffusion coefficient was more consistent with the same order of magnitude modeled for the ions in the small cells and the EU Directive experimental data sets (10^{-9} m^2 s^{-1}). The relatively higher velocity of the cations at this scale was related to the different pathways for the cations associated with the interlayer exchange positions of the smectites (Van Loon et al., 2007). In the landfill, sodium exchange was better simulated than the columns of the EU Directive. The higher concentration of sodium in the landfill leachate compared with the El Garráf leachate and the lower concentration of ammonium were responsible for the observed behavior. However, in addition to the occurrence of pure diffusion, the distribution of the solutes agreed with the significant mineralogical and physical changes in the landfill clay with increasing depth. The upper zone of the profile (<0.5-m depth) contained less clay and more carbonates, and the lower part (0.5-m depth) contained a more clay-like, compacted material. Apart from the scale effect, the natural and non-reworked clay at depths greater than 0.5 m performed better as a true natural barrier for the solutes that were highly concentrated in the upper part of the clay barrier.

4. Conclusions

Solute transport processes through a natural clay barrier were studied using a multi-scale approach. Conservative anion diffusion (chloride) was modeled at different scales. An order of magnitude of 10^{-10}–10^{-9} m^2 s^{-1} for the apparent diffusion coefficient was used to fit the chloride profiles at the different scales. However, at larger space and time scales, the transport velocity was retarded due to the presence of more consolidated, non-mechanically disturbed clay materials in the natural clay at different depths. The modeling of the cation transport was studied through cation exchange distribution variations. The modeling should be complemented using kinetic constraints to control the mineral dissolution. Calcium primarily dissolved from carbonates and silicates to achieve the chemical equilibrium conditions, which strongly buffered the distribution of the exchangeable cations. Thus, in most cases, it is difficult to accurately predict the migration profiles of sodium and ammonium.

The mixing of materials in the landfill base and the artificial compaction may produce a specific skin under the landfill, where the solutes are transported or retained. It is important to understand why this occurs for further studies of the clay materials so that these differences can be included in future models. The next step in this study is to better model the cation exchange and other reactions, such as the redox potential, which affects the dissolution-precipitation of minerals and organic evolution, to test the behavior of a more extended family of dissolved contaminants, including heavy metal ions.

Acknowledgments

This work was supported by the Spanish Environmental Ministry (MMA: I+D+i A113/2007/3_02.6) in cooperation with Geotecnia y Cimientos S.A. (GEOCISA), Centro de Experimentación de Obras Públicas (CEDEX), and the Instituto de Ciencias de la Tierra Jaume Almera (ICTJA).

References

Astudillo, J., 2001. El almacenamiento geológico profundo de los residuos radiactivos de alta actividad: principios básicos y tecnología. ENRESA, Madrid. 200 p.

Barone, F.S., Yanful, E.K., Quigley, R.M., Rowe, R.K., 1989. Effect of multiple contaminat migration on diffusion and adsorption of some domestic waste contaminant in a natural clayey soil. Canadian Geotechnical Journal 26, 189–198.

Bilitewski, B., Hardtle, G., Marek, K., Weissbach, A., Boeddicker, H., 1997. Waste Management. Springer, Berlin. 699 p.

Brindley, G.W., Brown, G., 1984. Crystal Structures of Clay Minerals and Their X-ray Identification. Mineralogical Society Pub, Great Britain. 495 p.

Brun, A., Engesgaard, P., 2002. Modelling of transport and biogeochemical processes in pollution plumes: literature review and model development. Journal of Hydrology 256, 211–227.

Cuevas, J., Leguey, S., Garralón, A., Rodríguez Rastrero, M., Procopio, J.R., Sevilla, Ma.T., Sánchez Jiménez, N., Rodríguez Abad, R., Garrido, A., 2009. Behavior of kaolinite and illite-based clays as landfill barriers. Applied Clay Science 42 (3–4), 497–509.

Davis, J.A., Kent, D.B., 1990. Surface complexation modelling in aqueous geochemistry. In: Hochella, M.F., White, A.F. (Eds.), Mineral-water Interface Geochemistry. Reviews in Mineralogy, vol. 23, pp. 177–248.

Derrington, D., Hart, M., Whitworth, T.M., 2006. Low head sodium phosphate and nitrate hyperfiltration through thin kaolinite and smectite layers—application to engineered systems. Applied Clay Science 33 (1), 52–58.

González, F., Gimmi, T., Juranvi, F., Van Loon, L., Diamond, L.W., 2009. Linking the diffusion of water in compacted clays at two different time scales: tracer through diffusion and Quasiealastic Neutron Scattering. Environmental Science and Technology 43, 3487–3493.

Hatch, B., 2008. Complex formation of acetic acid with Ca (II) and Mg (II), under physiological conditions. Journal of Solution Chemistry 37, 155–163.

Islam, J., Singhal, N., 2004. A laboratory study of landfill leachate transport in soils. Water Research 38, 2035–2042.

Malla, P.B., Douglas, L.A., 1987. Problems in identification of montmorillonite and beidellite. Clays and Clay Minerals 35, 232–236.

Michael, A., Malusis, M.A., Shackelford, D., 2002. Theory for reactive solute transport through clay membrane barriers. Journal of Contaminant Hydrology 59, 291–316.

Moore, D.M., Reynolds, R.C., 1989. X-ray Diffraction and the Identification and Analysis of Clay Minerals. Oxford University Press, Oxford. 378 p.

National Groundwater and Contaminated Land Center, 2003. Review of Ammonium Attenuation in Soil and Groundwater NGWCLC report NC/02/49.

Parkhurst, D.L., Appelo, C.A.J., 1999. User's Guide to PHREEQC (Version 2)—A Computer Program for Speciation, Batch Reaction, One-dimensional Transport, and Inverse Geochemical Calculations U.S. Geological Survey Water-Resources Investigations Report 99-4259, 312 p.

Pivato, A., Raga, R., 2006. Tests for the evaluation of ammonium attenuation in MSW landfill leachate by adsorption into bentonite in a landfill liner. Waste Management 26, 123–132.

Rhoades, J.D., 1982. Cation exchange capacity. In: Page, A.L., Miller, R.H., Keeney, D.R. (Eds.), Methods of Soil Analysis, part 2. Chemical and Microbiological Properties. Soil Science Society of America, 159–165. second ed.

Rogel, J.M., Leguey, S., Martínez de Santamaría, J.M., Cuevas, J., Muñoz, E., Garrido, A., Avellanosa, P., Hervás, J., Sevilla, MªT., Procopio, J.R., 2008. Proyecto de investigación y desarrollo sobre la evaluación del comportamiento de arcillas frente a lixiviados de vertederos urbanos. Subvenciones de I+D+i en el Ámbito de la prevención de la contaminación. Ministerio de Medioambiente. Gobierno de España, pp. 53–62.

Rowe, R., 1989. Movement of pollutants through clayey soil. In: Annual Geotechnical Conference. Minnesota Section ASCE, St. Paul, USA, pp. 1–34.

Rowe, R.K., Quigley, R.M., Booker, J.R., 1995. Clayey Barrier Systems for Waste Disposal Facilities. Spon Press, Abingdon, Oxon. 390 p.

Sawney, B.L., 1996. Sorption and desorption of organic contaminants by clays and soils. In: Sawney, B.L. (Ed.), Organic Pollutants in the Environment. CMS Workshop Lectures, vol. 8, pp. 45–69.

Savage, D., 1995. The Scientific and Regulatory Basis for the Geological Disposal of Radioactive Waste. John Willey and Sons Ltd, West Sussex. 437 p.

Sposito, G., 1990. Molecular models of ion adsorption on mineral surfaces. In: Hochella, M.F., White, A.F. (Eds.), Mineral-water Interface Geochemistry. Reviews in Mineralogy, vol. 23, pp. 261–278.

Stumm, W., 1992. Chemistry of the Solid-Water Interface. John Wiley & Sons, New York. 428 p.

Thomas, W.G., 1982. Exchangeable cations. In: Page, A.L., Miller, R.H., Keeney, D.R. (Eds.), Methods of Soil Analysis, Part 2, Chemical and Microbiological Properties. Soil Science Society of America, 159–165. second ed.

VanGulck, J.F., Rowe, R.K., Rittmann, B.E., Cooke, A.J., 2003. Predicting biogeochemical calcium precipitation in landfill collection systems. Biodegradation 14, 331–346.

VanGulck, J.F., Rowe, R.K., 2004. Evolution of clog formation with time in columns permeated with synthetic landfill leachate. Journal of Contaminant Hydrology 75, 115–139.

Van Loon, L.R., Glaus, M.A., Müller, W., 2007. Anion exclusion effects in compacted bentonites: towards a better understanding of anion diffusion. Applied Geochemistry 22, 2536–2552.

Williams, P.T., 1998. Waste Treatment and Disposal. John Willey and Sons, Chichester. 380 p.

Yanful, E.K., Nesbitt, H.W., Quigley, R.M., 1988a. Heavy metal migration at a landfill site, Sarnia, Ontario, Canada I: thermodynamic assessment and chemical interpretations. Applied Geochemistry 3 (5), 523–533.

Yanful, E.K., Nesbitt, H.W., Quigley, R.M., 1988b. Heavy metal migration at a landfill site, Sarnia, Ontario, Canada II: metal partitioning and geotechnical implications. Applied Geochemistry 3 (6), 623–629.